

Downscaling metawebs: propagation of uncertainties in species distribution and interaction probability

Gabriel Dansereau^{1,2,‡} Ceres Barros³ Timothée Poisot^{1,2}

¹ Université de Montréal ² Québec Centre for Biodiversity Sciences ³ University of British Columbia

‡ Equal contributions

Correspondance to:

Gabriel Dansereau — gabriel.dansereau@umontreal.ca

1 Introduction

2 Here, we present a method to downscale a metaweb in space by developing an explicit spatial probabilistic
3 metaweb for Canadian mammals. We present how the spatial structure of the downscaled metaweb varies in
4 space and how the uncertainty of interactions can be made spatially explicit. We further show that the
5 downscaled metaweb can highlight important biodiversity areas and bring novel ecological insights compared
6 to community measures.

7 Methods

8 Fig. 1 shows a conceptual overview of the methodological steps leading to the downscaled metaweb. The
9 components were grouped as the inputs (spatial or non-spatial), the localized steps (divided into
10 single-species-level, two-species-level, and network-level steps), and the final downscaled and spatialized
11 output. Throughout these steps, we highlight the importance of presenting the uncertainty of both interactions
12 and their distribution in space. We argue that this requires adopting a probabilistic view and incorporating
13 variation between scales.

14 [Figure 1 about here.]

15 Inputs

16 The inputs were divided into two main categories: the spatial and non-spatial ones (*Inputs* box on Fig. 1).

17 Non-spatial inputs

18 The main building block for the interaction data was the metaweb for Canadian mammals from Strydom *et al.*
19 (2022a), a non-spatial input (represented as nodes and links on Fig. 1). A metaweb contains all the possible
20 interactions between the species found in a given regional species pool (Dunne 2006). The species list for the
21 Canadian metaweb was extracted from the International Union for the Conservation of Nature (IUCN) checklist
22 (Strydom *et al.* 2022a). Briefly, the metaweb was developed using graph embedding and phylogenetic transfer
23 learning based on the metaweb of European mammals, which is itself based on a comprehensive survey of
24 interactions reported in the scientific literature (Maiorano *et al.* 2020). The Canadian metaweb is probabilistic,

25 which has the advantage of taking into account that species do not necessarily interact whenever they co-occur
26 (Blanchet *et al.* 2020). However, the Canadian metaweb is not explicitly spatial: it only gives information on
27 interactions in Canada as a whole and does not represent networks at specific locations. Local networks, on the
28 other hand, are realizations from the metaweb resulting from sorting the species and the interactions (Poisot *et*
29 *al.* 2015). A spatial and localized metaweb is not equivalent to the local networks, as it will have a different
30 structure and a higher connectance (Strydom *et al.* 2022b). Therefore, producing a spatial metaweb requires
31 additional steps to account for species composition and interaction variability in space.

32 **Spatial inputs**

33 The spatial data used to develop the spatial component of the metaweb were species occurrences and
34 environmental data. First, we extracted species occurrences from the Global Biodiversity Information Facility
35 (GBIF; www.gbif.org) for the Canadian mammals after reconciling species names between the Canadian
36 metaweb and GBIF using the GBIF Backbone Taxonomy (GBIF Secretariat 2021). Doing so, we removed
37 potential duplicates where species listed in the Canadian metaweb are considered as a single entity by GBIF. We
38 collected occurrences for our species list (159 species) using the GBIF download API on October 21st 2022
39 (GBIF.org 2022). We restricted our query to occurrences with coordinates between longitudes 175°W to 45°W
40 and latitudes 10°N to 90°N. This was meant to collect training data covering a broader range than our prediction
41 target (Canada only) and include observations in similar environments. Then, since GBIF observations
42 represent presence-only data and most predictive models require absence data, we generated pseudo-absence
43 data using the surface range envelope method available in `SimpleSDMLayers.jl` (Dansereau & Poisot 2021).
44 This method generates pseudo-absences by selecting random non-observed locations within the spatial range
45 delimited by the presence data (Barbet-Massin *et al.* 2012).

46 We used environmental data and species distribution models (SDMs, Guisan & Thuiller 2005) to predict the
47 distribution of Canadian mammals across the whole country. The environmental data we used were the 19
48 bioclimatic variables from CHELSA (Karger *et al.* 2017) and the 12 consensus land cover variables from
49 EarthEnv (Tuanmu & Jetz 2014). The CHELSA bioclimatic variables (*bio1-bio19*) represent various measures
50 of temperature and precipitation (e.g., annual averages, monthly maximum or minimum, seasonality) and are
51 available for land areas across the globe. Therefore, they can be used to capture the climatic tolerance of species
52 and model habitat suitability in new locations. We used the most recent version, the CHELSA v2.1 dataset
53 (Karger *et al.* 2021). However, this version also includes bioclimatic data for open water, while we decided here

54 to focus only on land surfaces. We used the previous version, CHELSA v1.2 (Karger *et al.* 2018), which shares
55 a similar grid but does not cover open water, as a mask to clip the v2.1 data to land surfaces only. The EarthEnv
56 land cover variables represent classes such as Evergreen broadleaf trees, Cultivated and managed vegetation,
57 Urban/Built-up, and Open Water. Values range between 0 and 100 and represent the consensus prevalence of
58 each class in percentage within a pixel. We coarsened both the CHELSA and EarthEnv data from their original
59 30 arc-second resolution to a 2.5 arc-minute one (around 4.5 km at the Equator) using GDAL/OGR
60 contributors (2021). This represented a compromise to catch both local variations and broad scale patterns
61 while limiting computation costs to a manageable level, as memory requirements on localized interactions rise
62 very quickly.

63 Our selection criteria for choosing an SDM algorithm was to have a method that generated probabilistic results,
64 including both a probability of occurrence for a species in a specific location and the uncertainty associated
65 with the prediction. These were crucial to obtaining a probabilistic version of the metaweb as they were used to
66 create spatial variations in the localized interaction probabilities (see next section). One promising method for
67 this is Gradient Boosted Trees with a Gaussian maximum likelihood from the `EvoTrees.jl` *Julia* package
68 (<https://github.com/Evoest/EvoTrees.jl>). This method returns a prediction for every pixel with an average value
69 and a standard deviation, which we used as a measure of uncertainty to build a Normal distribution for the
70 probability of occurrence of a given species at all pixels (represented as probability distributions on Fig. 1). We
71 trained models across the extent chosen for occurrences (longitudes 175°W to 45°W and latitudes 10°N to
72 90°N), then predicted species distributions only for Canada. We used the 2021 Census Boundary Files from
73 Statistics Canada (Statistics Canada 2022) to set the boundaries for our predictions, which gave us 970,698 sites
74 in total.

75 **Localized steps**

76 The next part of the method was the localized steps which produce local metawebs in every pixel. This
77 component was divided into single-species, two-species, and network-level steps (*Localized steps* box on Fig. 1).
78 The single-species steps represented four possible ways to account for uncertainty in the species distributions
79 and bring variation to the spatial metaweb. We explored four different options to select a value from the
80 occurrence distributions obtained in the previous steps (Inputs section): 1) taking the mean from the distribution
81 as the probability of occurrence (option 1 on Fig. 1); 2) converting the mean value to a binary one using a

specific threshold per species (option 2); 3) sampling a random value within the Normal distribution (option 3); 4) converting the random value into a binary result (option 4). The threshold (τ on Fig. 1) used was the value that maximized Youden's J informedness statistic (Youden 1950), the same metric used by Strydom *et al.* (2022a) at an intermediate step while building the metaweb. The four sampling options were intended to explore how uncertainty and variation in the species distributions can affect the metaweb result and reproduce some of the filterings that create the local network realizations (Poisot *et al.* 2015). We expected thresholding to have a more pronounced effect on network structure as it should reduce the number of links by removing many of the rare interactions (Poisot *et al.* 2016). Meanwhile, we expected random sampling to create spatial heterogeneity compared to the mean probabilities, as including some extreme values should disrupt the potential effects of environmental gradients.

Next, the two-species steps aimed to give the probability of observing a given interaction in a location. For all species pairs, we multiplied the two species' occurrence probability obtained using the sampling options described in the previous paragraph, then multiplied the co-occurrence probability by the interaction probability from the Canadian metaweb. For cases where species in the Canadian metaweb were considered as the same species by the GBIF Backbone Taxonomy (the reconciliation step mentioned earlier), we used the highest interaction probabilities involving the duplicated species.

The network-level steps then created the probabilistic metaweb for the location. We assembled all the local interaction probabilities (from the two-species steps) into a probabilistic network (Poisot *et al.* 2016). We then sampled several random network realizations to represent the potential local realization process (Poisot *et al.* 2015). Finally, this resulted in a distribution of localized networks, which we averaged over the number of simulations to obtain a probabilistic network.

Outputs

The final output of our method was the spatial probabilistic metaweb, which contains a localized probabilistic metaweb in every cell across the student extent (Outputs box on Fig. 1). This gives us an idea of the possible networks in all locations as the metaweb essentially serves to set an upper bound on the potential interactions (Strydom *et al.* 2022b), but with the added benefit of accounting for co-occurrence probabilities in this case. From there, we can create maps of network properties (e.g. number of links, connectance) measured on the local realizations, display their spatial distribution, and compute some community-level measures such as

species richness. We can also calculate the uncertainty associated with the network and community measurements and contrast their spatial distribution (see Supplementary Material).

Ecoregions

Since both species composition and network summary values display a high spatial variation and complex patterns, we simplified the representation of their distribution by grouping sites by ecoregion, as species and interaction composition have been shown to differ between ecoregions across large spatial scales (Martins *et al.* 2022). To do so, we used the global map of ecoregions from (Dinerstein *et al.* 2017; also used by Martins *et al.* 2022), rasterized it, and clipped it to Canada, which selected 44 different ecoregions. For every measure we report (e.g. species richness, number of links), we first calculated the measure for every site separately, then we extracted the median value for each ecoregion. We also measured the within-ecoregion variation by measuring the 89% interquantile range of the values in each ecoregion (threshold chosen to avoid confusion with conventional significance tests, inspired by McElreath 2020).

Ecological uniqueness

We compared the compositional uniqueness of the networks and the communities to verify if they indicated different exceptional areas. We measured uniqueness using the local contributions to beta diversity (LCBD, Legendre & De Cáceres 2013), which identify sites with exceptional composition by quantifying how much one site contributes to the total variance in the community composition. While many studies used LCBD values to evaluate uniqueness on local scales or few study sites (for example, da Silva & Hernández 2014; Heino & Grönroos 2017), recent studies used the measure on predicted species compositions over broad spatial extents and a large number of sites (Vasconcelos *et al.* 2018; Dansereau *et al.* 2022). LCBD values can also be used to measure uniqueness for networks by computing the values over the adjacency matrix, which has been shown to capture more unique sites and uniqueness variability than through species composition (Poisot *et al.* 2017). Here, we measured and compared the uniqueness of our localized community and network predictions. For species composition, we assembled a site-by-species community matrix with the probability of occurrence at every location from the species distribution models. For network composition, we assembled a site-by-interaction matrix with the localized interaction values from the spatial probabilistic metaweb. We applied the Hellinger transformation on both matrices and computed the LCBD values from the total variance in

the matrices (Legendre & De Cáceres 2013). High LCBD values indicate a high contribution to the overall variance and a unique species or interaction composition compared to other sites. Since values themselves are very low given our high number of sites (similar to Dansereau *et al.* 2022), what matters primarily is the magnitude of the difference between the sites. Given this, we divided values by the maximum value in each matrix (species or network) and suggest that these should be viewed as relative contributions compared to the highest observed contribution. As with other measures, we then summarized the local uniqueness values by ecoregion by taking the median LCBD value and measuring the 89% interquantile range within all ecoregions.

Software

We used *Julia* v1.9.0 (Bezanson *et al.* 2017) to implement all our analyses. We used packages `GBIF.jl` (Dansereau & Poisot 2021) to reconcile species names using the GBIF Backbone Taxonomy, `SpeciesDistributionToolkit.jl` to handle raster layers and species occurrences, `EcologicalNetworks.jl` (Poisot *et al.* 2019) to analyse network and metaweb structure, and `Makie.jl` (Danisch & Krumbiegel 2021) to produce figures. Our data sources (CHELSA, EarthEnv, Ecoregions) were all unprojected and we did not use a projection in our analyses, but we displayed the results using a Lambert conformal conic projection more appropriate for Canada using `GeoMakie.jl`. All the code used to implement our analyses is available on GitHub (<https://github.com/PoisotLab/SpatialProbabilisticMetaweb>) and includes instructions on how to run a smaller example at a coarse resolution. Note that running our analyses at full scale is resource and memory intensive and required the use of compute clusters provided by Calcul Québec and the Digital Research Alliance of Canada.

Results

Our method allowed us to display the spatial distribution of ecoregion-level measures (Fig. 2), either for community measures (e.g. expected species richness) or for network measures (e.g. expected number of links). Importantly, both community and network-level measures presented are not predictions of the measure itself but were instead computed over localized predictions of the communities and networks, then summarized for the ecoregions. Expected ecoregion richness (Fig. 2A), which is the median of the expected species richness of the sites within the ecoregion, and expected number of links (Fig. 2B) displayed similar distributions with a latitudinal gradient and higher values in the south. However, within-ecoregion variability was distributed differently, as some ecoregions along the coasts displayed higher interquantile ranges while ecoregions around

the southern border displayed narrower ones (Fig. 2C-D). All results shown are based on the first sampling strategy (option 1) mentioned in the Localized steps section, where species occurrence probabilities were taken as the mean value of the distribution (results for other sampling strategies are discussed in Supplementary Material).

[Figure 2 about here.]

Direct comparison of the spatial distributions of species richness and expected number of links showed some areas with mismatches, both regarding the median estimates and regarding the within-ecoregion variability (Fig. 3). Median values for the ecoregions showed a similar bivariate distribution with ecoregions in the south mostly displaying high species richness and a high number of links (Fig. 3A). The northernmost ecoregions (Canadian High Artic Tundra and Davis Highlands Tundra) displayed higher richness (based on the quantile rank) compared to the number of links. Inversely, ecoregions further south (Canadian Low Artic Tundra, Northern Canadian Shield Taiga, Southern Hudson Bay Taiga) ranked higher for the number of links than for species richness. On the other hand, within-ecoregion variability showed different bivariate relationships and a less constant latitudinal gradient (Fig. 3B). This indicates that richness and link do not vary hand in hand (i.e. their variability is not closely connected) although they may show similar distributions for median values.

[Figure 3 about here.]

Our results also indicate a mismatch between the uniqueness of communities and networks (Fig. 4). Uniqueness was higher mostly in the north and along the south border for communities, but only in the north for networks (Fig. 4A-B). Consequently, ecoregions with both unique community composition and unique network composition were mostly in the north (Fig. 4C). Meanwhile, some areas were unique for one element but not the other. For instance, the New England-Acadian forests ecoregion (south-east, near 70°W and 48°N) had a highly unique species composition but a more common network composition (Fig. 4C). Opposite areas with unique network compositions only were higher north between latitudes 52°N and 70°N (Eastern Canadian Shield Taiga, Northern Canadian Shield Taiga, Canadian Low Artic Tundra). When comparing the values, network uniqueness values for ecoregions spanned a narrower range between the 44 ecoregions than species LCBD values (Fig. 4D, left). Within-ecoregion variation was also lower for network values with generally lower 89% interquantile ranges among the site-level LCBD values (Fig. 4D, right). Moreover, mismatched sites (unique for only one element) formed two distinct groups when evaluating the relationship between species richness and the

number of links (see Supplementary Material). The areas only unique for their species composition had both a high richness and number of links. On the other hand, the sites only unique for their networks had both lower richness and a lower number of links, although they were not the sites with the lowest values for both.

[Figure 4 about here.]

Discussion

The spatial probabilistic metaweb we produced here is a first attempt at downscaling a metaweb and producing localized predictions, as called for by Strydom *et al.* (2022b). It gives us an idea of what local metawebs or networks could look like in space, given the species distributions and their variability, as well as the uncertainty around the interactions. It is the first representation in space of the metaweb of Canadian mammals (Strydom *et al.* 2022a), which is not spatialized. Conceptually, this is similar to how the European tetrapod metaweb (Maiorano *et al.* 2020) was used to predict localized networks in Europe (Braga *et al.* 2019; O'Connor *et al.* 2020; Galiana *et al.* 2021; Gaüzère *et al.* 2022; Botella *et al.* 2023). Therefore, our approach could open similar possibilities of investigations in North America with food webs of Canadian mammals, for instance on the structure of food webs over space (Braga *et al.* 2019), on the scaling of network area relationships (Galiana *et al.* 2021), and on the effect of land-use intensification on food webs (Botella *et al.* 2023). Moreover, our approach is probabilistic, does not assume species interact whenever they co-occur, and incorporates variability based on environmental conditions, which could lead to different results by introducing a different association between species richness and network properties. Galiana *et al.* (2021) found that species richness had a large explanatory power over network properties but mentioned it could potentially be due to interactions between species being fixed in space. Here, we found mismatches in the distribution of species richness and interactions, and especially regarding their within-ecoregion variability (Fig. 3), highlighting that interactions might vary differently than species distributions in space. Network measures (links on Fig. 3A) were also lower in the north, contrarily to previous studies (e.g. connectance higher in the north, Braga *et al.* 2019; Galiana *et al.* 2021). Our LCBD and uniqueness results highlighted that areas with unique network composition might differ from sites with unique species composition. In other words, the joint distribution of community and network uniqueness highlights different diversity hotspots. Poisot *et al.* (2017) showed a similar result with host-parasite communities of rodents and ecto-fleas. Our results further show how these differences could be distributed across ecoregions and a broad spatial extent. Areas unique for only one element (species or network

220 composition) differed in their combination of species richness and number of links (supplementary material),
221 with species-unique sites displaying high values of both measures and network-unique sites displaying low
222 values. Moreover, LCBD scores essentially highlight variability hotspots and are a measure of the variance of
223 community or network structure. Here they also serve as an inter-ecoregion variation measure which can be
224 compared to the within-ecoregion variation highlighted by the interquantile ranges. The narrower range of
225 values for network LCBD values and the lower IQR values indicate that both the inter-ecoregion and
226 within-ecoregion variation are lower for network than for species (Fig. 4). Additionally, higher values for
227 network LCBD also indicate that most ecoregions can hold ecologically unique sites.

References

- Barbet-Massin, M., Jiguet, F., Albert, C.H. & Thuiller, W. (2012). [Selecting pseudo-absences for species distribution models: How, where and how many?](#) *Methods in Ecology and Evolution*, 3, 327–338.
- Bezanson, J., Edelman, A., Karpinski, S. & Shah, V.B. (2017). [Julia: A fresh approach to numerical computing.](#) *SIAM Review*, 59, 65–98.
- Blanchet, F.G., Cazelles, K. & Gravel, D. (2020). [Co-occurrence is not evidence of ecological interactions.](#) *Ecology Letters*, 23, 1050–1063.
- Botella, C., Gaüzère, P., O'Connor, L., Ohlmann, M., Renaud, J., Dou, Y., *et al.* (2023). [Land-use intensity influences European tetrapod food-webs](#) (Preprint). Preprints.
- Braga, J., Pollock, L.J., Barros, C., Galiana, N., Montoya, J.M., Gravel, D., *et al.* (2019). [Spatial analyses of multi-trophic terrestrial vertebrate assemblages in Europe.](#) *Global Ecology and Biogeography*, 28, 1636–1648.
- da Silva, P.G. & Hernández, M.I.M. (2014). [Local and regional effects on community structure of dung beetles in a mainland-island scenario.](#) *PLOS ONE*, 9, e111883.
- Danisch, S. & Krumbiegel, J. (2021). [Makie.jl: Flexible high-performance data visualization for Julia.](#) *Journal of Open Source Software*, 6, 3349.
- Dansereau, G., Legendre, P. & Poisot, T. (2022). [Evaluating ecological uniqueness over broad spatial extents using species distribution modelling.](#) *Oikos*, 2022, e09063.
- Dansereau, G. & Poisot, T. (2021). [SimpleSDMLayers.jl and GBIF.jl: A framework for species distribution modeling in Julia.](#) *Journal of Open Source Software*, 6, 2872.
- Dinerstein, E., Olson, D., Joshi, A., Vynne, C., Burgess, N.D., Wikramanayake, E., *et al.* (2017). [An Ecoregion-Based Approach to Protecting Half the Terrestrial Realm.](#) *BioScience*, 67, 534–545.
- Dunne, J. (2006). The network structure of food webs. In: *Ecological Networks: Linking Structure to Dynamics in Food Webs*. pp. 27–86.
- Galiana, N., Barros, C., Braga, J., Ficetola, G.F., Maiorano, L., Thuiller, W., *et al.* (2021). [The spatial scaling of food web structure across European biogeographical regions.](#) *Ecography*, 44, 653–664.

254 Gaüzère, P., O'Connor, L., Botella, C., Poggiato, G., Münkemüller, T., Pollock, L.J., *et al.* (2022). [The diversity](#)
 255 [of biotic interactions complements functional and phylogenetic facets of biodiversity](#). *Current Biology*.

256 GBIF Secretariat. (2021). [GBIF Backbone Taxonomy](#).

257 GBIF.org. (2022). [GBIF occurrence download](#).

258 GDAL/OGR contributors. (2021). *GDAL/OGR geospatial data abstraction software library*. Manual. Open
 259 Source Geospatial Foundation.

260 Guisan, A. & Thuiller, W. (2005). [Predicting species distribution: Offering more than simple habitat models](#).
 261 *Ecology Letters*, 8, 993–1009.

262 Heino, J. & Grönroos, M. (2017). [Exploring species and site contributions to beta diversity in stream insect](#)
 263 [assemblages](#). *Oecologia*, 183, 151–160.

264 Karger, D.N., Conrad, O., Böhner, J., Kawohl, T., Kreft, H., Soria-Auza, R.W., *et al.* (2017). [Climatologies at](#)
 265 [high resolution for the earth's land surface areas](#). *Scientific Data*, 4, 170122.

266 Karger, D.N., Conrad, O., Böhner, J., Kawohl, T., Kreft, H., Soria-Auza, R.W., *et al.* (2018). [Data from:](#)
 267 [Climatologies at high resolution for the earth's land surface areas](#).

268 Karger, D.N., Conrad, O., Böhner, J., Kawohl, T., Kreft, H., Soria-Auza, R.W., *et al.* (2021). [Climatologies at](#)
 269 [high resolution for the earth's land surface areas](#).

270 Legendre, P. & De Cáceres, M. (2013). [Beta diversity as the variance of community data: Dissimilarity](#)
 271 [coefficients and partitioning](#). *Ecology Letters*, 16, 951–963.

272 Maiorano, L., Montemaggiore, A., Ficetola, G.F., O'Connor, L. & Thuiller, W. (2020). [TETRA-EU 1.0: A](#)
 273 [species-level trophic metaweb of European tetrapods](#). *Global Ecology and Biogeography*, 29, 1452–1457.

274 Martins, L.P., Stouffer, D.B., Blendinger, P.G., Böhning-Gaese, K., Buitrón-Jurado, G., Correia, M., *et al.*
 275 (2022). [Global and regional ecological boundaries explain abrupt spatial discontinuities in avian frugivory](#)
 276 [interactions](#). *Nature Communications*, 13, 6943.

277 McElreath, R. (2020). *Statistical rethinking: A bayesian course with examples in R and Stan*. Second.
 278 Chapman and Hall/CRC, New York.

279 O'Connor, L.M.J., Pollock, L.J., Braga, J., Ficetola, G.F., Maiorano, L., Martinez-Almoyna, C., *et al.* (2020).
 280 [Unveiling the food webs of tetrapods across Europe through the prism of the Eltonian niche](#). *Journal of*

281 *Biogeography*, 47, 181–192.

282 Poisot, T., B  lisle, Z., Hoebeke, L., Stock, M. & Szefer, P. (2019). [EcologicalNetworks.jl: Analysing ecological](#)
283 [networks of species interactions](#). *Ecography*, 42, 1850–1861.

284 Poisot, T., Cirtwill, A.R., Cazelles, K., Gravel, D., Fortin, M.-J. & Stouffer, D.B. (2016). [The structure of](#)
285 [probabilistic networks](#). *Methods in Ecology and Evolution*, 7, 303–312.

286 Poisot, T., Gu  veneux-Julien, C., Fortin, M.-J., Gravel, D. & Legendre, P. (2017). [Hosts, parasites and their](#)
287 [interactions respond to different climatic variables](#). *Global Ecology and Biogeography*, 26, 942–951.

288 Poisot, T., Stouffer, D.B. & Gravel, D. (2015). [Beyond species: Why ecological interaction networks vary](#)
289 [through space and time](#). *Oikos*, 124, 243–251.

290 Statistics Canada. (2022). *Boundary files, reference guide second edition, Census year 2021*. Second edition.
291 Statistics Canada = Statistique Canada, Ottawa.

292 Strydom, T., Bouskila, S., Banville, F., Barros, C., Caron, D., Farrell, M.J., *et al.* (2022a). [Food web](#)
293 [reconstruction through phylogenetic transfer of low-rank network representation](#). *Methods in Ecology and*
294 *Evolution*, n/a.

295 Strydom, T., Bouskila, S., Banville, F., Barros, C., Caron, D., Farrell, M.J., *et al.* (2022b). [Predicting metawebs:](#)
296 [Transfer of graph embeddings can help alleviate spatial data deficiencies](#).

297 Tuanmu, M.-N. & Jetz, W. (2014). [A global 1-km consensus land-cover product for biodiversity and ecosystem](#)
298 [modelling](#). *Global Ecology and Biogeography*, 23, 1031–1045.

299 Vasconcelos, T.S., Nascimento, B.T.M. do & Prado, V.H.M. (2018). [Expected impacts of climate change](#)
300 [threaten the anuran diversity in the Brazilian hotspots](#). *Ecology and Evolution*, 8, 7894–7906.

301 Youden, W.J. (1950). [Index for rating diagnostic tests](#). *Cancer*, 3, 32–35.

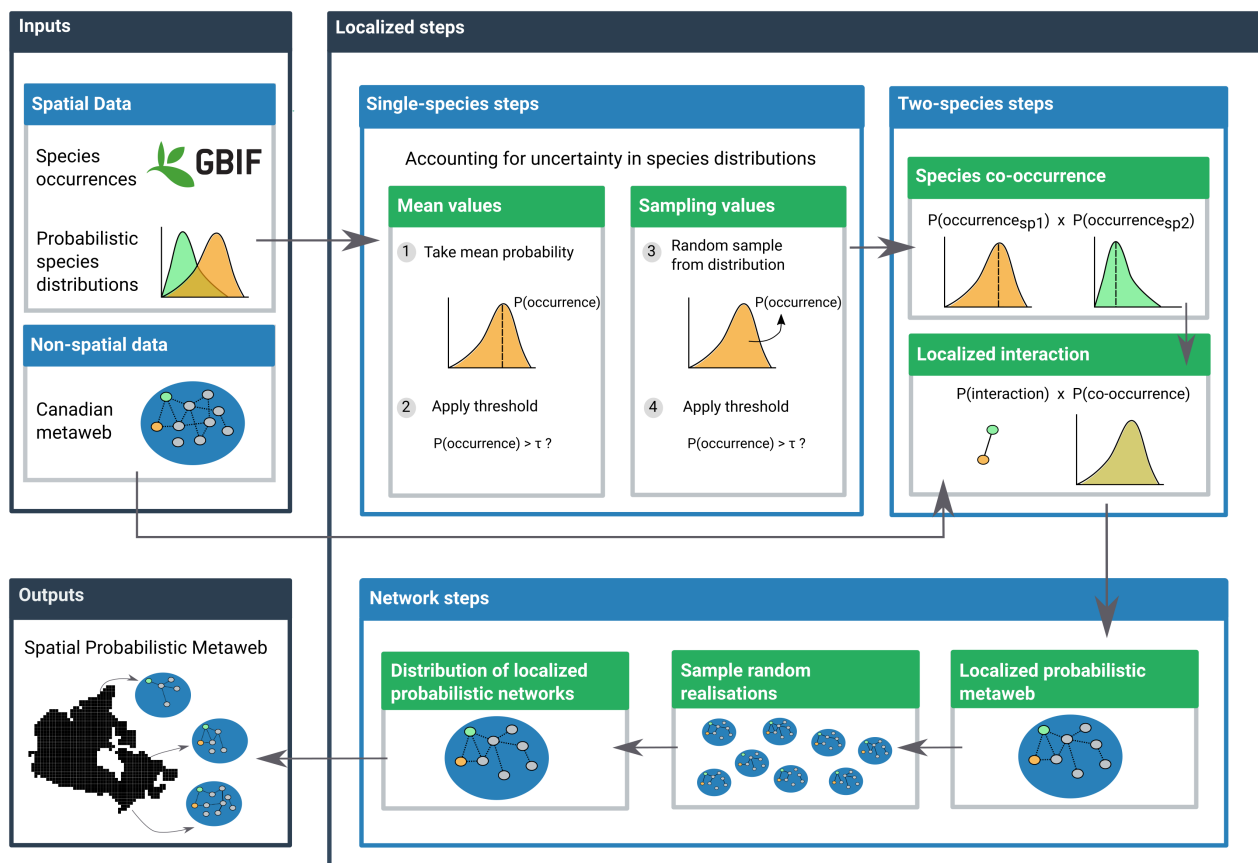


Figure 1: Conceptual figure of the workflow to obtain the spatial probabilistic metaweb (Chapter 1). The workflow has three components: the inputs, the localized steps, and the final spatial output. The inputs are composed of the spatial data (data with information in every cell) and the non-spatial data (constant for all of Canada). The localized steps use these data and are performed separately in every cell, first at a single-species level (using distribution data), then for every species pair (adding interaction data from the metaweb), and finally at the network level by combining the results of all species pairs. The final output coming out of the network-level steps contains a spatialized probabilistic metaweb for every cell across the study extent.

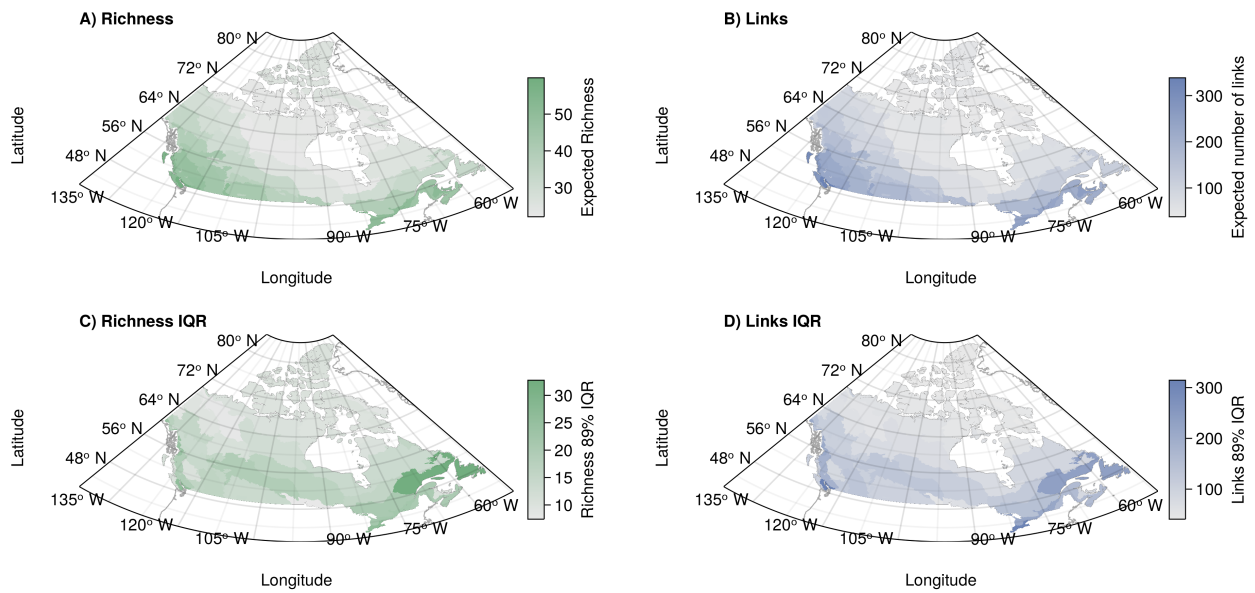


Figure 2: (A-B) Example of a community measure (A, expected species richness) and a network one (B, expected number of links). Both measures are assembled from the predicted probabilistic communities and networks, respectively. Values are first measured separately for all sites, then the median value is taken to represent the ecoregion-level value. (C-B) Representation of the 89% interquantile range of values within the ecoregion for expected richness (C) and expected number of links (D).

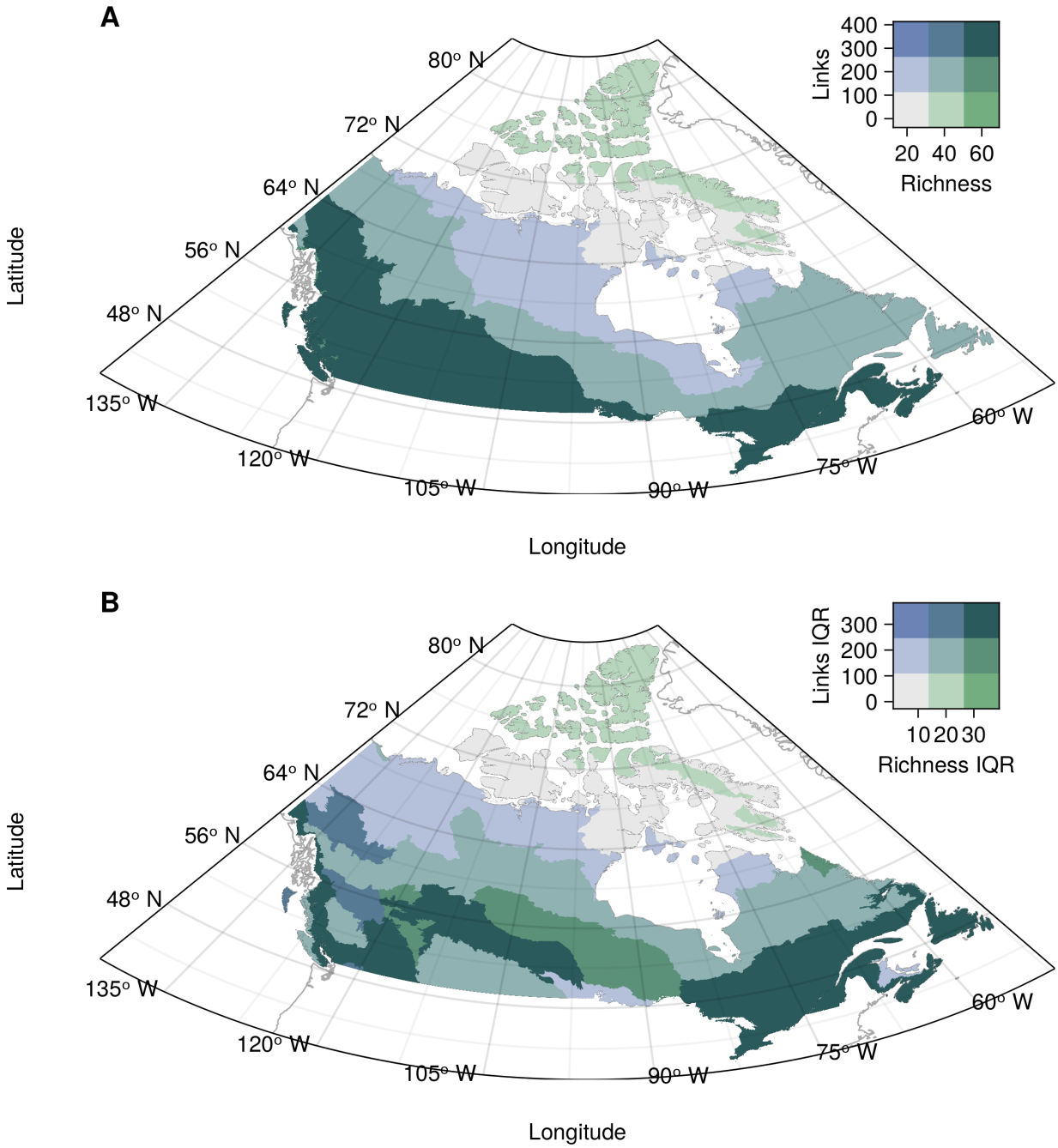


Figure 3: Bivariate relationship between community and network measures for the median ecoregion value (A) and the within-ecoregion 89% interquantile range (B). Values are grouped into three quantiles separately for each variable. The colour combinations represent the nine possible combinations of quantiles. Species richness (horizontal axis) goes left to right from low (light grey, bottom left) to high (green, bottom right). The number of links goes bottom-up from low (light grey, bottom left) to high (blue, top left).

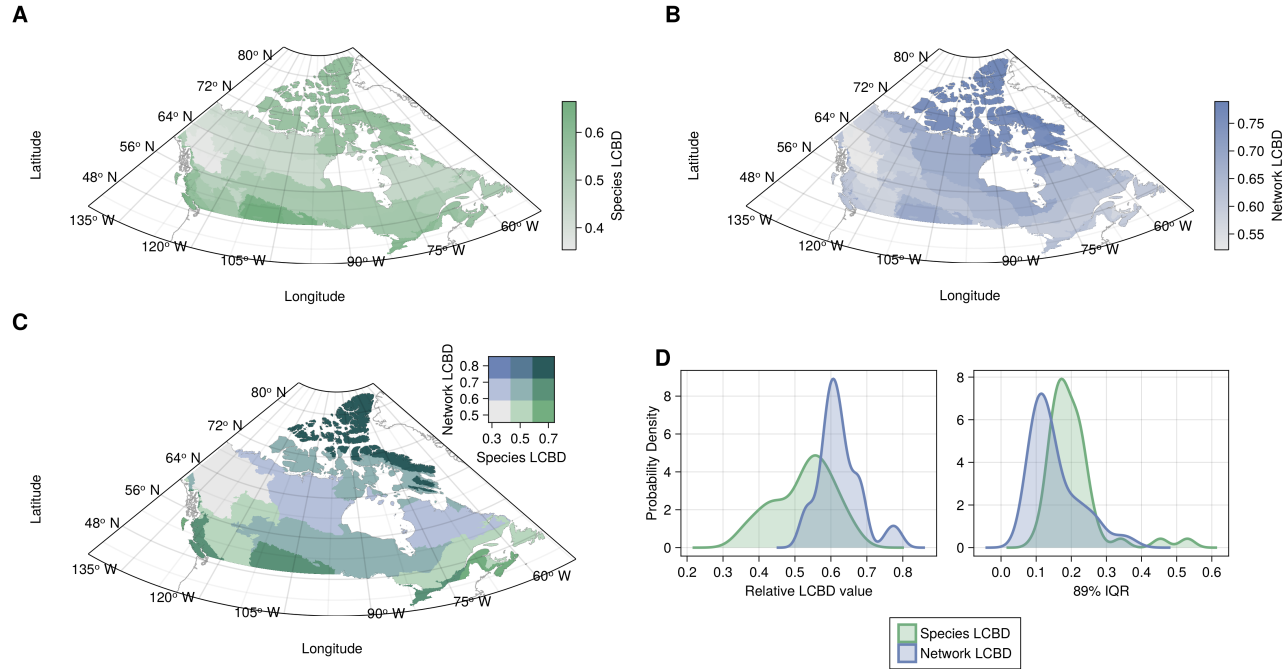


Figure 4: (A-B) Representation of the ecoregion uniqueness values based on species composition (a) and network composition (b). LCBD values were first computed across all sites and scaled relative to the maximum value observed. The ecoregion LCBD value is the median value for the sites in the ecoregion. (C) Bivariate representation of species and network composition LCBD. Values are grouped into three quantiles separately for each variable. The colour combinations represent the nine possible combinations of quantiles. The species uniqueness (horizontal axis) goes left to right from low uniqueness (light grey, bottom left) to high uniqueness (green, bottom right). The network composition uniqueness goes bottom-up from low uniqueness (light grey, bottom left) to high uniqueness (blue, top left). (D) Probability densities for the ecoregion LCBD values for species and network LCBD (left), highlighting the variability of the LCBD between ecoregions, and the 89% interquartile range of the values within each ecoregion (right), highlighting the variability within the ecoregions.